

# Model-based Thermal Anomaly Detection in Cloud Datacenters

Eun Kyung Lee, Hariharasudhan Viswanathan, and Dario Pompili

NSF Cloud and Autonomic Computing Center

Department of Electrical and Computer Engineering, Rutgers University, New Brunswick

e-mail: {eunkyung\_lee, hari\_viswanathan, pompili} @cac.rutgers.edu

**Abstract**—The growing importance, large scale, and high server density of high-performance computing datacenters make them prone to strategic attacks, misconfigurations, and failures (cooling as well as computing infrastructure). Such unexpected events lead to thermal anomalies – hotspots, fugues, and coldspots – which significantly impact the total cost of operation of datacenters. A model-based thermal anomaly detection mechanism, which compares expected (obtained using heat generation and extraction models) and observed thermal maps (obtained using thermal cameras) of datacenters is proposed. In addition, a Thermal Anomaly-aware Resource Allocation (TARA) scheme is designed to create time-varying thermal fingerprints of the datacenter so to maximize the accuracy and minimize the latency of the aforementioned model-based detection. TARA significantly improves the performance of model-based anomaly detection compared to state-of-the-art resource allocation schemes.

**Keywords**—Anomaly detection, heat imbalance, virtualization.

## I. INTRODUCTION

High-Performance Computing (HPC) systems housed in datacenters are a key component of the society's IT infrastructure. Due to their growing importance, datacenters are strategic targets [1] for *denial-of-service attacks* (running illegitimate workloads) and *cooling system attacks* aimed at causing thermal runaways and, hence, costly outages, which can potentially cripple critical health, banking and commerce, defense, scientific research, and educational infrastructures. Furthermore, due to their large scale and high server density, the probability of computing and cooling system misconfigurations as well as of cooling equipment and server fan failures is high [2]. Such unpredictable events may result in unexpected high temperature areas/regions (hotspots) or excessively cooled low temperature areas/regions (coldspots) also referred to as *thermal anomalies*.

Local unevenness in heat-generation (by computing and communication equipment) and heat-extraction (by cooling equipment) rates determines the temperature distribution inside a datacenter. The heat-generation and -extraction rates may differ, which over time leads to what we call *heat imbalance* [3]. Unexpected changes in the local heat-generation and -extraction rates due to 1) attacks (on the computing or cooling infrastructure), 2) Computer Room Air Conditioning (CRAC) unit and server fan failures, and/or 3) computing and cooling system misconfigurations may over time cause an unexpected large positive heat imbalance resulting in a significant temperature increase and, hence, in unexpected thermal hotspots. Such hotspots may also result in thermal *fugues*, which are characterized by a continuous increase in the rate of temperature rise. Thermal anomalies such as unexpected hotspots and fugues lead to system operation in unsafe temperature regions [4], which will increase the server failure

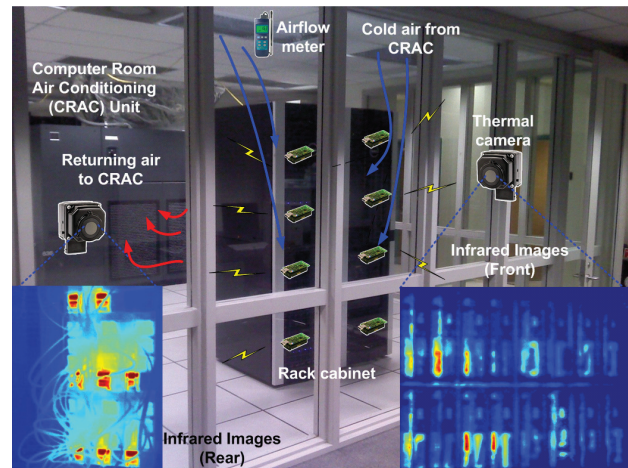


Fig. 1. Multi-tier sensing infrastructure composed of temperature and humidity sensors, airflow meters, and thermal cameras for thermal-aware datacenter management.

rate. Computing as well as cooling system misconfigurations may also cause energy-inefficient overcooling resulting in unexpected coldspots. In summary, thermal anomalies, i.e., hotspots, fugues, and coldspots, significantly impact the Total Cost of Ownership (TCO) of datacenters.

Thermal awareness, i.e., the knowledge of heat imbalance (for a given distribution of workloads at different regions inside a datacenter), is essential for timely detection and classification of thermal anomalies so to minimize their effect on the efficiency, availability, security, and lifetime of mission-critical HPC systems. In [5], we proposed a multi-tier sensing infrastructure (composed of temperature and humidity sensors, airflow meters, and thermal cameras as shown in Fig. 1) for autonomic management of datacenters (i.e., self-organizing, self-optimizing, and self-healing), and in [3], we designed and validated a simple yet robust heat-imbalance model, which exploits the data from the sensing infrastructure. The notion of heat imbalance allows us to predict future temperature maps of the datacenter and take proactive management decisions such as workload placement [3] and cooling system optimization [6].

In this paper, we propose an efficient method for online (real-time) processing and interpretation of infrared images (also called thermograms) with the knowledge of heat imbalance at various regions inside a datacenter for thermal anomaly detection. State of the art in thermal anomaly detection in datacenters involves complex offline processing of thermograms in order to construct 2-D (two dimensional) or 3-D reconstruction

of thermal maps of datacenters for detailed visual inspection by domain experts [7], [8], [9] and to identify electrical, mechanical, computing, and/or cooling system faults. On the contrary, we decompose thermograms from thermal cameras with a large field of view in to localized sub-images by exploiting our prior knowledge of the *aisle-rack-enclosure-blade layout* in order to focus on specific Regions of Interest (ROIs). Our anomaly detection scheme is *model-based*, i.e., it involves comparison of *expected* (generated using the heat-imbalance model) and *observed* (obtained from thermograms) thermal maps.

In addition to model-based thermal anomaly detection, in this paper, we propose a Thermal Anomaly-aware Resource Allocation (TARA) solution, which exploits the knowledge of heat imbalance. Our idea is to create a time-varying thermal fingerprint (thermal map) of the datacenter so that the intensity of an unexpected hotspot is sufficiently high for the model-based detection to notice (even when a very low detection threshold is used). TARA allocates workloads or Virtual Machines (VMs, in case of a virtualized datacenter) to servers where the heat imbalance due to the workload is high in order to maximize the temperature difference between two consecutive thermal maps. This strategy allows for early detection of failures (as the solution tries to utilize as many servers as possible) and easy detection of attacks (such as illegitimate workloads).

In summary, our contributions in this paper include:

- A model-based approach to thermal anomaly detection in HPC cloud datacenters that involves comparison of expected and observed thermal maps.
- TARA, an anomaly-aware resource allocation solution for virtualized datacenters, which significantly improves the accuracy of our model-based anomaly detection technique.

Creation of consecutive thermal maps that vary significantly from each other (for early and easy detection of anomalies) is possible when there is no cap on power usage. No cap on the power budget implies unlimited access to additional servers and no restriction on costly workload migrations, which are unrealistic. Hence, we assume that TARA operates under strict power budgets and it is designed to factor in the costs of operating additional servers and of workload migrations while maximizing the detection accuracy for a given power budget. TARA can significantly contribute to the thermal anomaly detection (7%, 15%, and 31% average improvement in thermal anomaly detection with only 10% false positive rate) compared to the traditional scheduling algorithms: random, round robin, and best-fit-decreasing.

The remainder of this paper is organized as follows: in Sect. II, we present the state of the art in thermal anomaly detection in cloud datacenters; in Sect. III, we discuss our proposed solution for thermal anomaly detection along with a anomaly- and energy-aware virtual machine allocation solution, which significantly improves the detection accuracy; in Sect. IV, we explain our evaluation methodology and the observations from our simulation study; finally, in Sect. V we present our conclusion with a brief note on future work.

## II. STATE OF THE ART

Traditional methods for anomaly detection, which rely on aggregation (at a monitor node) and on continuous online analysis of huge amounts of data (e.g., job requests and distribution, server utilization, network traffic, internal sensor values, etc.), are prohibitive in a large datacenter because of limitations in terms of network bandwidth and computational overhead. In addition, such methods are incapable of detecting thermal anomalies as they do not capture the complex thermodynamic phenomena inside a datacenter. Hence, we propose to extract information from the raw measured data (using an external sensing infrastructure as shown in Fig. 1) and to create knowledge about the heat imbalance and impart self-protection capabilities on large-scale HPC systems.

Even though an external, heterogeneous, network of point-source sensors (e.g., temperature and humidity scalar sensors, and air flow meters) could help capture complex thermodynamic phenomena, such a network would not scale in terms of overhead (communication, computation, and energy) and cost when the size of the datacenter and its server density increase significantly (consider instrumenting a large HPC datacenter consisting of 1000 racks and 50 blade servers in each rack). The amount of sensed information collected and processed every second at a monitor node would be of the order of gigabits. It is important to note that not all data is significant, which creates the need for it to be prioritized in terms of the value of information that can be obtained. Hence, we introduce the use of thermal cameras, which have a large field of view and can provide temperature distribution information at a greater granularity than scalar point-source temperature sensors through remote sensing.

In [10], the authors propose four methods to perform ‘prediction’ or ‘early detection’ of thermal anomalies so to enable proactive thermal management decisions. The first three methods are variants of a simple temperature-threshold-based approach, while the fourth method employs a Bayesian classifier to ‘predict’ thermal anomalies. The threshold-based methods rely heavily on the choice of the threshold and the time window used for classification of events as either normal or anomalous. Of the four proposed methods, the Bayesian classifier method performs best by predicting thermal anomalies earlier than the rest while also minimizing false positives. However, this Bayesian method takes only scalar temperature measurements as inputs, involves an offline training phase, does not use models, and finally does not provide insights into the causes and locations of the anomalies: for these reasons appropriate preemptive steps cannot be taken immediately. In contrast, we incorporate data from a heterogeneous sensing infrastructure [5], [11], [12] into models to profile thermally a datacenter in space and time, and then exploit this information for early thermal-anomaly detection by comparing it against appropriate features extracted from raw thermal images.

Recently, datacenter managers have started using infrared thermography to locate and diagnose problems such as short cycling of the air conditioning system, loose electrical connections, worn out wires, and fan failures [7], [8], [9]. These solutions rely heavily on manual inspection of thermal images to detect anomalies. On the contrary, our thermal anomaly detection solution employs knowledge of workload distribution and multi-modal sensor data in the heat-imbalance model as

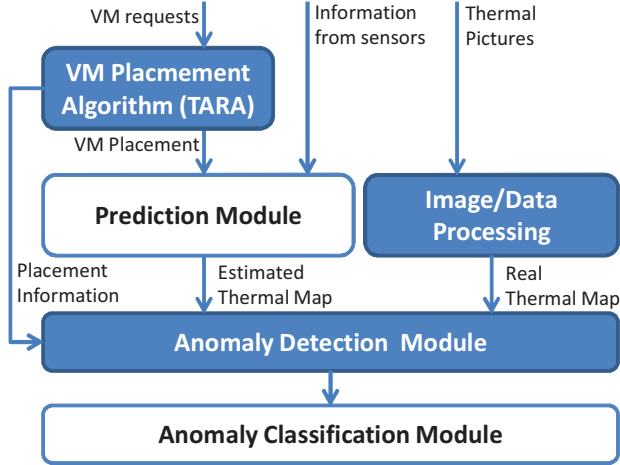


Fig. 2. The different modules that make up our thermal anomaly detection solution (the focus of this paper is indicated in blue boxes).

well as infrared thermograms to automatically detect thermal anomalies through comparison of expected and observed thermal maps. Prior work on thermal management of datacenters target either the *uptime-conscious datacenter managers*, who are interested in eliminating hotspots (for security, reliability, and availability), or the *energy-conscious datacenter managers*, who are interested in eliminating coldspots (for energy efficiency). In contrast, our solution for thermal-aware resource allocation, TARA, is bestowed with controllable parameters that allow the datacenter managers to exploit the energy vs. anomaly-detection accuracy tradeoff.

### III. PROPOSED SOLUTION

The overall scope of our work is shown in Fig. 2. Our solution is composed of four main modules: VM placement (resource allocation), prediction (heat-imbalance estimation), image/data processing (thermography), and anomaly detection (comparison) modules. The VM placement module includes TARA, which allocates physical resources to the VMs in such a way that the detection accuracy is maximized for a given power budget. The prediction module uses the VM placement information and other sensor information to estimate the thermal map. Then, the model-based anomaly detection module compares the estimated thermal map with the observed thermal map (processed by image/data processing module) to detect anomalies. Firstly, we elaborate on our heat-imbalance model for the estimation of expected thermal map. Secondly, we present how we extract thermal maps from thermograms in our solution. Finally, we formulate thermal anomaly-aware resource allocation as an optimization problem aimed at maximizing the anomaly detection probability, and propose a heuristic that balances the energy-accuracy tradeoff.

#### A. Expected Thermal Map

A VM is created for every application request and is provisioned with resources (CPUs, memory, disk, and network capacity) that satisfy the application requirements (usually deadline). Without any loss of generality, we assume that this provisioning has already been performed using techniques such

as the ones described in [13]. The provisioned VMs now have to be allocated to physical servers housed within racks in datacenters. Let  $\mathcal{M}$  be the set of VMs to be allocated and  $\mathcal{N}$  be the set of servers. An associativity binary matrix  $\mathbf{A} = \{a_{mn}\}$  (with  $a_{mn} \in \{0, 1\}$ ) specifies whether VM  $m$  is hosted at server  $n$  or not. A VM  $m$  is specified as a vector  $\mathbf{\Gamma}_m = \{\gamma_m^s\}$ , where  $s \in \mathcal{S} = \{CPU, MEM, IO, NET\}$  refers to the server subsystems and  $\gamma_m^s$ 's are the VM subsystem requirements (e.g., CPU cores, amount of volatile memory [MB], disk storage space [MB], network capacity [Mbps]).

Representation (or *mapping*) of a VM's subsystem requirement ( $\gamma_m^s$ ) as a factor of physical server subsystem capacity is straightforward if all the servers of the datacenter are assumed to be homogeneous. For example, a VM  $m$  requiring 4 virtual CPUs, 2GB of RAM, 64GB of hard-disk space, and 100Mbps network capacity can be represented as  $\mathbf{\Gamma}_m = \{0.25, 0.125, 0.125, 0.1\}$  if all the servers in a datacenter have 16 CPU cores, 16GB of RAM, 512GB of local hard-disk space, and a gigabit ethernet interface. The mapping problem becomes non trivial in an heterogeneous environment. However, assuming that only a small finite number of generations of each subsystem are present in the datacenter, we create such a mapping for each generation of every subsystem.

*Heat imbalance:* In our previous work [3], we formulated the heat-imbalance model in a datacenter based on heat-generation ( $h_n$ ) and heat-extraction ( $q_n$ ) rates as follows,

$$\Delta I_n = \int_{t_0}^{t_0+\delta} (h_n - q_n) dt = M_n \cdot C \cdot \Delta T_{[t_0, t_0+\delta]}^n, \quad (1)$$

where  $\Delta I_n$  [J] denotes the heat imbalance of CPU inside server  $n$  during the time between  $t_0$  and  $t_0 + \delta$ , and  $M_n$  and  $C$  denote the mass and specific heat capacity, respectively, of the CPU. Note that if  $\Delta I_n$  is positive (i.e.,  $h_n > q_n$ ), the temperature of the CPU at server  $n$  increases in the time interval  $[t_0, t_0 + \delta]$  (hence,  $\Delta T^n > 0$ ); conversely, if  $\Delta I_n$  is negative (i.e.,  $h_n < q_n$ ), the temperature of the CPU at server  $n$  decreases (hence,  $\Delta T^n < 0$ ). This estimated heat imbalance helps us generate the expected thermal map of the datacenter as long as the information about the different workloads and their potential location (physical server) as well as real-time temperature and airflow measurement are known.

#### B. Observed Thermal Map

Infrared thermograms are used to acquire accurate thermal maps of the datacenter. As the thermogram gives high resolution current temperature map, we can extract more information (i.e., size, intensity, degree) about thermal hotspots than what we can using scalar sensors. Even though the thermogram includes denser information (each pixel indicates the temperature of certain location) than a scalar sensor measurement, the estimation algorithm could be readily over fitted giving wrong estimation if the ROIs of the thermogram and the image features are not properly selected.

*Regions of Interest:* We decompose thermograms from thermal cameras with a large field of view to localized sub-images in order to focus on specific ROIs (e.g., racks, enclosures, servers, and fans). This decomposition allows for fast diagnosis of thermal anomalies through comparison of localized thermal maps of ROIs with the estimated thermal

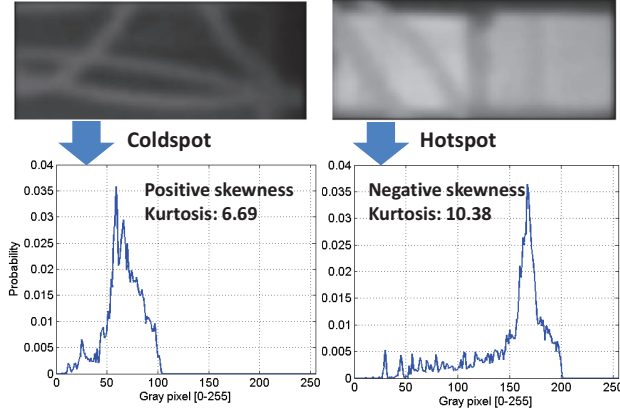


Fig. 3. Histogram analysis of thermal images capturing a coldspot on an idle server (left) and a hotspot on a 70% utilized server (right).

maps from the heat-imbalance model. Our proposed solution does not require accurate 2-D or 3-D thermal maps of the entire datacenters.

**Histogram Analysis:** The output of a thermal camera is a gray scale image formed using infrared radiation from an object. Image pixels indicate temperature measures of different points on the object’s surface. We employ higher-order histogram statistics as they convey information about not only the intensity of the image pixels (temperature) but also their distribution. Histogram is a graphical representation of the ‘distribution’ of data (pixel values). The statistics are obtained by first getting the histogram of pixel values from an  $N \times M$  sub-image matrix  $I$ , which has been processed using a median blurring filter as well as a Gaussian blurring filter, to remove the noise. We then calculate an empirical probability density function  $p(x)$  (where  $0 \leq x \leq 255$ ) from the relative frequencies of each pixel in the sub-image. Figure 3 shows the pdf of pixel intensities in an image of server fan vents under two different settings, idle and 70% CPU utilization.

Through histogram analysis, abstracted features (intensity, size, and distribution) about hotspots and coldspots can be determined. For example, the pixels in the right-most value indicates the hottest temperature in the thermogram and the left-most value indicates the coldest temperature. In the same way, the mean, median, maximum, and minimum values extracted from the histogram convey the size of the hotspot and/or coldspot. In addition, higher-order statistics provide insights into the distribution of hotspots and/or coldspots. Using the standard notation to denote  $p(x)$ ’s moments-about-the-mean and the standard deviation, we calculate the following higher-order histogram statistics, skewness and kurtosis [14].

Extraction of skewness and kurtosis allows us to determine how to interpret the pixel values to get the best representation of the temperature inside the server. Skewness and kurtosis help us understand whether a thermal image has a hotspot or a coldspot and how big it is, respectively. Skewness gives information regarding the asymmetry of the histogram. Positive skewness indicates presence of a coldspot as there are more pixels in low temperature (Fig. 3 left), and negative skewness indicates presence of a hotspot as there are more pixels in high temperature (Fig. 3 right). The high absolute value of

the skewness also indicates high intensity of the hotspot or coldspot. The kurtosis gives information about the “peakedness” of the histogram, which in turn represents the size of the hotspot or the coldspot. Thus, more accurate representation of the temperature can be extracted by jointly employing the skewness and kurtosis.

### C. Thermal Anomaly-aware Resource Allocation: TARA

We propose a novel VM allocation solution (TARA), which increases the probability of detecting unexpected hotspots (thermal anomalies) when the number of computing resources that can be operational for a given load (set of workload requests) is increased. TARA harnesses information from our sensing infrastructure (thermal cameras, airflow meters, and internal sensors), the VM requests, and the prediction module (heat imbalance model) to allocate VMs such that the orthogonality between two consecutive thermal maps. Then, the original thermal map, captured online, is compared with the predicted one using our heat-imbalance model [3] and the seed numbers to detect anomalous VM placement.

**Energy-accuracy Tradeoff:** Our novel anomaly-aware resource allocation method enables self-protection by inducing as much difference between consecutive thermal maps (generated every  $\delta$  seconds) as possible given the budget ( $\beta$ ), which restricts the number of servers that can be utilized in the datacenter. Parameter  $\beta$  represents the fraction of total datacenter resources that can be used and the corresponding power budget is given by,  $P_\beta = P_{max} \cdot \beta$ , where  $P_{max}$  is the power consumption when all the computing resources are utilized to the maximum in the datacenter. The higher the power budget, the greater the number of servers that can be utilized, and hence, the greater the difference between thermal maps (resulting in a higher detection rate). TARA allows the datacenter managers to exploit the budget  $\beta$  to explore the tradeoff between energy expenditure and anomaly detection accuracy. Note that  $\beta$  is always greater than  $\beta_0$ , which is the minimum fraction of resources in the datacenter that is required for a given set of workloads to be completed without compromising their quality of service.

Figure 4(a) shows an actual enclosure of eight servers. Figure 4(b) shows an example temperature map at time  $t_0$  and thermal map change from time  $t_0$  to  $t_0 + \delta$  under different power budgets (Figs. 4(c) and 4(d)). For the scenario depicted in Fig. 4,  $\beta_0$  is 0.375. The difference between the thermal maps at  $t_0$  and  $t_0 + \delta$  can be increased by increasing the budget  $\beta$ . Here, the difference between thermal maps at  $t_0$  and  $t_0 + \delta$  are  $30^\circ C$  and  $48^\circ C$  for  $\beta = 0.5$  (Fig. 4(c)) and  $\beta = 0.75$  (Fig. 4(d)), respectively.

An uptime-conscious datacenter manager may be interested in eliminating hotspots so to increase service availability (and hence, use a high  $\beta$ ). An energy-conscious datacenter manager, on the other hand, may be interested in eliminating coldspots so to improve energy efficiency (and hence, use a low  $\beta$ ). TARA can autonomously allocate resources within the budget that the datacenter manager provides. Our VM allocation solution changes the thermal map when allocating resources to VMs every  $\delta$  seconds. The moving target in the thermal domain (varying thermal map) increases the robustness of our anomaly detection module. We first formulate the VM

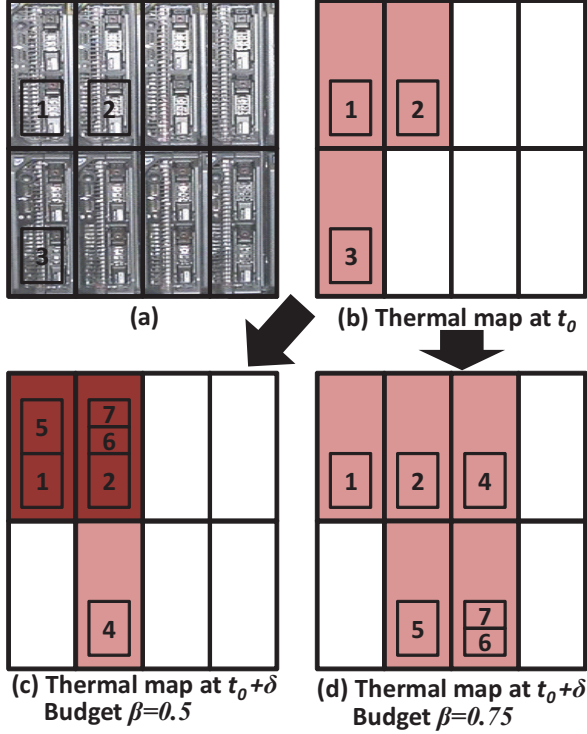


Fig. 4. Toy example of VM allocation using TARA with different budgets ( $\beta = 0.5, 0.75$ ): (a) An actual enclosure with eight blade-servers; (b) Thermal map of an enclosure at  $t_0$  with three active VMs; A possible allocation of four newly arrived VMs (4 to 7) and the corresponding thermal map at  $t_0 + \delta$  (c) when the budget  $\beta = 0.5$  ( $\beta_0 = 0.375$ ) and (d) when the budget  $\beta = 0.75$  ( $\beta_0 = 0.375$ ). Note that VM 3 is not shown in (c) and (d) as it is assumed to have ended right after  $t_0$ . Thermal anomalies due to attacks can be easily detected and the ones due to failures can be detected early when the budget  $\beta = 0.75$  as opposed to the case when  $\beta = 0.5$  because the expected hotspots' intensities are kept low.

allocation problem as an optimization problem, which employs our heat-imbalance model. The motivation for formulating the optimization problem is to gain insight and make key design decisions for our heuristic solution.

**Optimization Problem:** The goal is to find an *optimal* mapping of VMs to physical servers (represented by the binary associativity matrix  $\mathbf{A}$ ) so to maximize the difference between the existing thermal map and the expected thermal map (5) when the workloads in the VMs are all active. The known (given as well as measured) parameters and optimization variables of the optimization problem can be summarized as,

- Given (offline)** :  $\mathcal{N}, T^{reco}, \delta, M_n, C_p;$   
**Given (online)** :  $\beta_0, \beta, \mathcal{M}, \Gamma_m \forall m \in \mathcal{M};$   
**Measured (online)** :  $T_n^{t_0}, m_n^{in}, T_n^{in}, \Lambda_n \forall n \in \mathcal{N};$   
**Find** :  $\mathbf{A} = \{a_{mn}\}, m \in \mathcal{M}, n \in \mathcal{N}. \quad (2)$

Here,  $T_n^{t_0}$  and  $\Lambda_n = \{\lambda_n^s\}$  represent the current CPU temperature and the maximum residual capacity of each subsystem  $s$  at server  $n$ , respectively. The objective of the optimization

problem is,

$$\text{Maximize : } \sum_{n \in \mathcal{N}} |T_n^{t_0} - \tilde{T}_n^{t_0+\delta}|; \quad (3)$$

**Subject to : C1, C2, C3, C4.**

Here,  $\tilde{T}_n^{t_0+\delta} = T_n^{t_0} + \Delta T_{[t_0, t_0+\delta]}^n$  is the estimated temperature of an "active" server  $n$  at time  $t_0 + \delta$  and  $\Delta T_{[t_0, t_0+\delta]}^n$  is calculated using (3). If the server is unused, then we set  $\Delta T_{[t_0, t_0+\delta]}^n = 0$ . The first constraint,

$$\text{C1: } \sum_{n \in \mathcal{N}} a_{mn} = 1, \forall m \in \mathcal{M}, \quad (4)$$

ensures that a VM is allocated to *one* and *only one* server. The second constraint,

$$\text{C2: } \sum_{m \in \mathcal{M}} a_{mn} \cdot \gamma_m^s \leq \lambda_n^s, \forall n \in \mathcal{N}, \forall s \in \mathcal{S}, \quad (5)$$

ensures that the resource requirements of all VMs allocated to one server do not exceed the maximum capacity of a server subsystem. The third constraint,

$$\text{C3: } T_n^{t_0} + \Delta T_{[t_0, t_0+\delta]}^n \leq T^{reco}, \forall n \in \mathcal{N}, \quad (6)$$

ensures that the predicted CPU temperature – sum of the current CPU temperature  $T_n^{t_0}$  and the predicted temperature increase  $\Delta T_{[t_0, t_0+\delta]}^n$  calculated using the heat-imbalance model – is always below the recommended maximum operating temperature ( $T^{reco}$ ), which is chosen by the datacenter manager. The fourth constraint,

$$\text{C4: } \beta_0 \leq \frac{\sum_{n \in \mathcal{N}} r_n}{|\mathcal{N}|} \leq \beta, \forall n \in \mathcal{N}, \quad (7)$$

ensures that the specified utilization factor of the datacenter (in terms of number of active servers) is not exceeded. Here,  $r_n$  is an indicator variable that conveys whether a server  $n$  is active or not,

$$r_n = \begin{cases} 1 & \text{if } \sum_{m \in \mathcal{M}} a_{mn} \geq 1 \\ 0 & \text{otherwise} \end{cases}, \forall n \in \mathcal{N}. \quad (8)$$

This optimization problem is NP-hard as it needs to find the maximum temperature difference when allocating  $|\mathcal{M}|$  workloads to  $|\mathcal{N}|$  servers (combinatorial problem). Hence, we present our heuristic solution in Algo. 1,

**Algorithm 1** TARA: Thermal Anomaly-aware Resource Allocation.

```

INIT:
 $P_s = \{\text{Maximum power required to run a server}\}$ 
 $P_\beta = \{\text{Power budget [W]}\}$ 
 $N_{PS} = \{\text{Potential number of servers to run VM}\}$ 
VM_ALLOCATION:
Calculate  $N_{PS}$  given the power budget  $P_\beta$  allowed,  $P_\beta > N_{PS} \cdot P_s$ 
for  $i = 1 \rightarrow \text{length}(\mathcal{M})$  do
  Find server  $j \in \mathcal{N}$ , where the heat imbalance is maximal but CPU temp. is less than  $T^{reco}$ 
  Place  $i$ th VM to the server  $j$ 
end for

```

The objective of TARA (maximize the temperature difference to maximize the detection accuracy) is in line with the objective of the optimization problem, i.e., the more the active physical servers, greater the detection accuracy. This is also

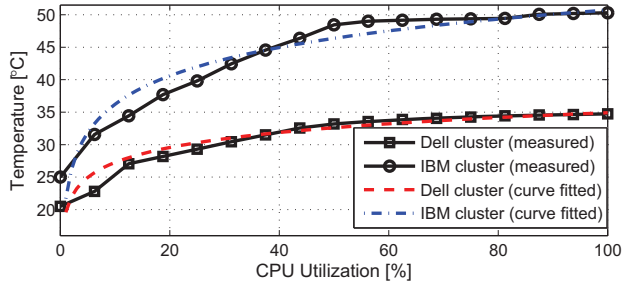


Fig. 5. Relationship between temperature and CPU utilization using data from both RU and UFL servers.

made possible due to the logarithmic behavior (as shown in Fig. 5) of CPU temperature with respect to CPU utilization in multi-core multi-threaded systems which are measured using two different platforms, Dell cluster (PowerEdge M620 blade server) and IBM cluster (blade center) at Rutgers University (RU) and University of Florida (UFL) machine rooms (which are the most common computing equipment configuration in cloud datacenters). As the temperature difference is smaller when utilizing higher number of cores, the detection rate decreases under high utilization (at each server).

#### IV. PERFORMANCE EVALUATION

We evaluated the performance of TARA, in terms of thermal-anomaly-detection accuracy, via experiments on a small-scale testbed, and via trace-driven simulations. We performed small-scale experiments (16 servers) to design large-scale simulations (220 servers) under realistic assumptions. The system model used in our simulations has the same characteristics of our real testbed (e.g., temperature profile of CPU, room temperature, and workload profile). First, we provide details on our testbed and experiment methodology (workload traces, performance metrics, and competing approaches). Then, we elaborate on the simulation scenarios aimed at highlighting the benefits of anomaly-aware VM allocation for efficient anomaly detection.

##### A. Testbed and Simulation Methodology

*Testbed:* We have a fully equipped machine room in NSF CAC at RU with state-of-the-art computing equipment (modern blade servers in enclosures) and a fully controllable CRAC system. The blade servers are equipped with a host of internal sensors that provide information about server subsystem operating temperatures and utilization. In addition, the machine room at RU is instrumented with an external heterogeneous sensing infrastructure [5] to capture the complex thermodynamic phenomena of heat generation and extraction at various regions inside the machine room. The sensing infrastructure comprises of scalar temperature and humidity sensors placed at the server inlet (cold aisle) and outlet (hot aisle), airflow meters at the server outlet, and thermal cameras in the hot aisle.

The computing equipment configuration is two Dell M1000E modular blade enclosures. Each enclosure is maximally configured with sixteen blades, each blade having two Intel Xeon E5504 Nehalem family quad-core processors at 2.0 GHz, forming an eight core node. Each blade has 6 GB RAM

and 80 GB of local disk storage. The cluster system consists of 32 nodes, 256 cores, 80 GB memory and 2.5 TB disk capacity. The cooling equipment is a fully controllable Liebert 22-Ton Upflow CRAC system.

*Workloads:* We used real HPC production workload traces from the RIKEN Integrated Cluster of Clusters (RICC) [15]. The trace included data from a massively parallel cluster, which has 1024 nodes each with 12 GB of memory and two 4-core CPUs. As the RICC is a large-scale distributed system composed of a large number of nodes, we scaled and adapted the job requests to the characteristics of our system model. First, we converted the input traces to the Standard Workload Format (SWF) [16]. Then, we eliminated failed and canceled jobs as well as anomalies. As the traces did not provide all the information needed for our analysis, we needed to complete them using a model based on [17]. The entire trace consists of 400,000 requests spread over 6 months. The trace used in our simulation have 5,200 requests spread over 2 days.

*Competing Strategies:* We compared the performance of TARA against four strategies, namely, Random, Round Robin (RR), Best-Fit-Decreasing (BFD), and an energy-plus-thermal-aware consolidation technique VMAP [3]. In Random, the VMs are allocated in random sequence to any server. In RR, the VMs are allocated sequentially to servers. In BFD, the VMs are sorted according to volume. Then, each VM is allocated to the first physical server (w.r.t. server ID), which not only satisfies all the four subsystem utilization requirements but also has the least residual volume after packing that VM. In VMAP, VM is allocated to minimize the energy consumption while ensuring that the servers do not overheat.

*Metrics:* We evaluate the impact of our approach in terms of the following metrics: True Positive Rate (TPR) and False Positive Rate (FPR) of anomalies, and *energy consumption* (in kilowatt-hour [kWh]). TPR and FPR are depicted using *Receiver Operating Characteristic (ROC)* [18] curves. The TPR and FPR are calculated using different thresholds and the resulting points are plotted as a ROC curve. The larger the area under ROC curve, the better the performance of the detection in terms of accuracy.

Figure 6(a) shows ROC of TARA and competing algorithms. When the budget is high enough, TARA outperforms other competing algorithm. Random placement and RR show higher detection rate than VMAP and BFD because they inherently spread the VMs like TARA does resulting in a large number of lightly-loaded servers in which unexpected hotspots can easily be identified. However, VMAP and BFD consolidate VMs making the temperature map change due to anomalous events insignificant, resulting in low detection rate. Thus, energy consumption shown in Fig. 6(b) of VMAP and BFD is lower than TARA, VMAP, RR, and Random as they save a significant amount of energy by turning of the unused servers. TARA's anomaly-detection-rate is higher than those of other non-consolidation schemes even though its energy consumption is comparable to others'.

We performed simulations to see the impact of uncertainty in data reported by the hardware sensors on the detection rate. Figure 6(c) shows ROC of TARA with different degrees of sensor-data uncertainty. As our heat imbalance model uses the temperature measurement we generate the Gaussian noise with

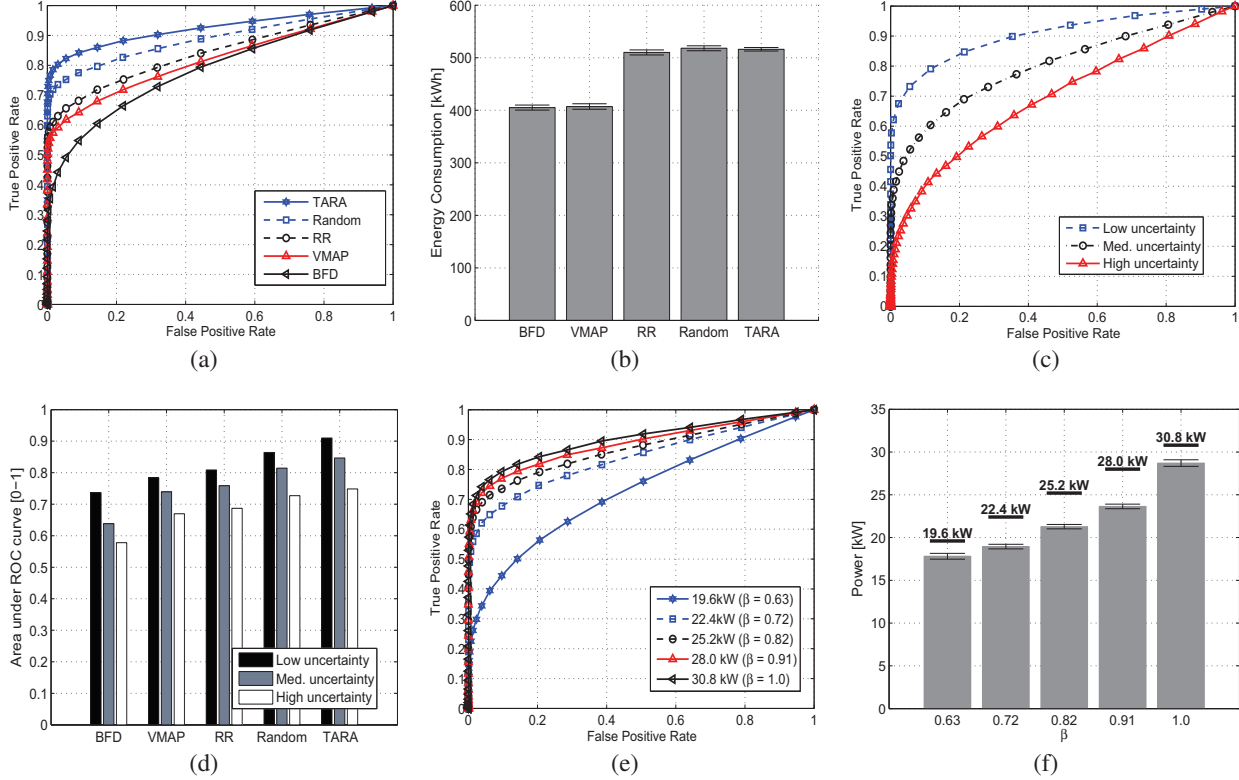


Fig. 6. (a) ROC of TARA with competing algorithms; (b) Energy consumption of TARA with competing algorithms; (c) ROC of TARA with different degree of uncertainty; (d) Area under ROC of TARA with different degree of uncertainty; (e) ROC of TARA with different power budget (here,  $\beta_0 = 0.55$ ); (f) Average power level of TARA with different power budget.

TABLE I. INTENSITY AND DISTRIBUTION OF THERMAL ANOMALIES

Causes of Thermal Anomaly		Intensity	Distribution
Attack	DOS attack	High	Group
	SPY VM	Low	Sporadic
Failure	CRAC fan	High	Group
	Server fan	High	Sporadic
Misconfig.	Misplacement	Normal	Diff. from Orig.
	Profiling Error	Diff. from Orig.	Normal

the same mean ( $\mu = 0^\circ C$ ), but different standard deviations ( $\sigma = 0.5, 2.5, \text{ and } 4.5^\circ C$ , for low, medium, high environment uncertainties, respectively). The performance of model-based anomaly detection drops when uncertainty increases because our heat-imbalance model cannot perform well when the input is too noisy. Figure 6(d) shows the bar graph of area under ROC curve with different algorithms. The area under ROC curve of TARA's is higher than that of other schemes' representing higher detection accuracy for different degrees of uncertainty.

Figure 6(e) shows the ROC of TARA under different power budgets. Detection accuracy improves with increase in the power budget as more servers are available to distribute the workload and to maximize the difference between consecutive thermal maps (the objective of TARA). This Figure 6(f) shows average power usage given the power budget. It shows that instead of exploiting the entire power budget TARA explores the solution space to find the most power efficient configuration that can provide the highest possible detection accuracy for

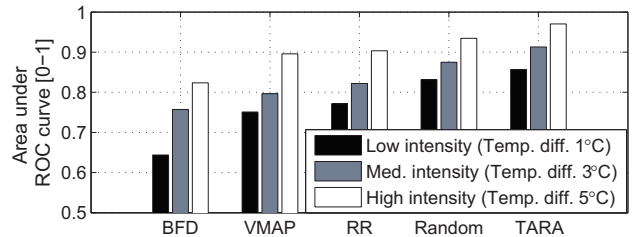


Fig. 7. Area under ROC of TARA and competing algorithms in the presence of anomalies of different intensities.

a given power budget. Figure 7 shows the ROC of TARA given anomalies of different intensities. As the intensity and the distribution of unexpected hotspots caused by different types anomalies can be different as summarized in Table I, we designed simulations with anomalies of different intensities (1, 3, and  $5^\circ C$ , for low, medium, and high intensity, respectively). Our model-based anomaly detection mechanism in conjunction with TARA performs the best under all scenarios. It shows that the detection rate increase when the anomaly intensity increases even when a low threshold is used in our model-based anomaly detection mechanism.

*Discussion:* Let us take a brief look at how the detection rate can be further improved if TARA has knowledge about the average workload duration and VM migration capability. By Little's theorem, we can estimate the average number of

VMs in the datacenter if we know the average arrival rate of the VM requests and the average life time of the VMs. For a given arrival rate, when the average life time of the VMs is very low (less than  $\delta$ ), then the thermal maps created every  $\delta$  as a result of VM placement (using TARA or any other mechanism) will be significantly different from their predecessors' by default. When the average life time of the VMs is comparable to  $\delta$ , then the difference between consecutive thermal maps can be increased by increasing the budget  $\beta \geq \beta_0$  as it will allow the use of previously unused servers. Note that placing a VM in a freshly started server results in a higher increase in temperature than the one in an already active server. This is possible due to the logarithmic increase of server temperature with utilization shown in Fig. 5.

However, when the average life time of the VMs is high compared to  $\delta$ , then the average number of VMs at any point in time in the datacenter will be very high. Under such circumstances,  $\beta_0 \simeq 1$  and  $\beta$  cannot be increased further. The only way the detection rate can be increased (especially for attacks such as spy VMs) is by migrating the high-intensity hotspots to various regions inside the datacenter. This "hopping" of high-intensity hotspots in space and time makes it a moving target problem for attackers. Remember that servers with higher utilization rates and longer duration VMs are suitable targets for attackers as their spy VMs may go undetected (they will incur only a very small temperature increase in highly utilized servers).

## V. CONCLUSIONS

Anomalies (i.e., attacks, misconfigurations, hardware failures) are becoming a significant concern for the datacenter managers as the failure of detecting them can cost a large business millions of dollars in losses. Our model-based thermal anomaly detection solution in conjunction with TARA can significantly improve the detection probability (7%, 15%, and 31% average improvement in detection with only 10% false positive rate) compared to model-based anomaly detection with traditional scheduling algorithms: random, round robin, and best-fit-decreasing.

## VI. ACKNOWLEDGEMENTS

This work was supported in part by the National Science Foundation, under grants CNS-0855091, IIP-0758566, and CNS-1117263.

## REFERENCES

- [1] J. Jung, B. Krishnamurthy, and M. Rabinovich, "Flash crowds and denial of service attacks: Characterization and implications for cdns and web sites," in *Proc. of the Intl. Conference on World Wide Web (WWW)*, Honolulu, HI, May 2002.
- [2] R. Zhou, Z. Wang, C. E. Bash, T. Cade, and A. McReynolds, "Failure resistant data center cooling control through model-based thermal zone mapping," in *Proc. of ASME Summer Heat Transfer Conference (HT)*, Puerto Rico, USA, 2012.
- [3] E. K. Lee, H. Viswanathan, and D. Pompili, "VMAP: Proactive Thermal-aware Virtual Machine Allocation in HPC Cloud Datacenters," in *Proc. of the IEEE Intl. Conference on High Performance Computing (HiPC)*, Pune, India, Dec. 2012.
- [4] J. Srinivasan, S. V. Adve, P. Bose, and J. A. Rivers, "The Impact of Technology Scaling on Lifetime Reliability," in *Proc. of the International Conference on Dependable Systems and Networks (DSN)*, Jun. 2004.
- [5] H. Viswanathan, E. K. Lee, and D. Pompili, "Self-organizing Sensing Infrastructure for Autonomic Management of Green Datacenters," *IEEE Network*, vol. 25, no. 4, pp. 34–40, Jul. 2011.
- [6] E. K. Lee, I. Kulkarni, D. Pompili, and M. Parashar, "Proactive Thermal Management in Green Datacenter," *Journal of Supercomputing (Springer)*, vol. 60, no. 2, pp. 165–195, May 2012.
- [7] Stockton Infrared Thermographic Services, "Using thermal mapping at the data center," <http://www.stocktoninfrared.com/using-thermal-mapping-at-the-data-center/>.
- [8] Energex Technologies, "Datacenter thermal imaging and analysis," [http://energextech.com/Data\\_Center\\_Thermal.pdf](http://energextech.com/Data_Center_Thermal.pdf).
- [9] Electronic Environments Infrastructure Solutions, "Why thermal imaging of your data center infrastructure is important?" <http://www.eecnet.com/Resources/Articles/Why-Thermal-Imaging-for-Power-Cooling-Infrastruc/>.
- [10] M. Marwah, R. Sharma, and C. Bash, "Thermal anomaly prediction in data centers," in *Proc. of IEEE Intersociety Conference on Thermal and Thermomechanical Phenomena in Electronic Systems (ITherm '10)*, Las Vegas, NV, Jun. 2010.
- [11] R. R. Schmidt, K. Karki, K. Kelkar, A. Radmehr, and S. Patankar, "Measurements and Predictions of the Flow Distribution through Perforated Tiles in Raised Floor Data Centers," in *Proc. of Pacific Rim/ASME International Electronic Packaging Technical Conference (IPACK)*, Kauai, HI, 2001.
- [12] R. R. Schmidt, "Thermal Profile of a High-Density Data Center-Methodology to Thermally Characterize a Data Center," *American Society of Heating, Refrigerating and Air-Conditioning Engineers (ASHRAE) Transactions*, vol. 110, no. 2, pp. 635–642, 2004.
- [13] I. Rodero, J. Jaramillo, A. Quiroz, M. Parashar, F. Guim, and S. Poole, "Energy-efficient Application-aware Online Provisioning for Virtualized Clouds and Data Centers," in *Proc. of Intl. Green Computing Conference (GREENCOMP)*, Chicago, IL, Aug. 2010.
- [14] R. M. Haralick, K. Shanmugam, and I. Dinstein, "Textural features for image classification," *Systems, Man and Cybernetics, IEEE Transactions on*, vol. SMC-3, no. 6, pp. 610–621, Nov. 1973.
- [15] The RIKEN Integrated Cluster of Clusters (RICC) Log. [Online]. Available: [http://www.cs.huji.ac.il/labs/parallel/workload/l\\_ricc/index.html](http://www.cs.huji.ac.il/labs/parallel/workload/l_ricc/index.html)
- [16] D. Feitelson, "Parallel Workload Archive," 2010. [Online]. Available: <http://www.cs.huji.ac.il/labs/parallel/workload/>
- [17] U. Lublin and D. G. Feitelson, "The Workload on Parallel Supercomputers: Modeling the Characteristics of Rigid Jobs," *Journal of Parallel Distributed Computing*, vol. 63, no. 11, pp. 1105–1122, Nov. 2003.
- [18] J. Kerekes, "Receiver Operating Characteristic Curve Confidence Intervals and Regions," *Geoscience and Remote Sensing Letters*, vol. 5, no. 2, pp. 251–255, Apr. 2008.